Published in final edited form as:
Prostate. 2014 February ; 74(2): . doi:10.1002/pros.22737.

p62/SQSTM1 is required for cell survival of apoptosis-resistant bone metastatic prostate cancer cell lines

Megan A. Chang[1], **Micaela Morgado**[1], **Curtis R. Warren**[1], **Cimona V. Hinton**[2], **Mary C. Farach-Carson**[1], and **Nikki A. Delk**[1]

[1]Department of Biochemistry and Cell Biology, Rice University, BioScience Research Collaborative, 6500 Main, MS 601, Houston, TX 77030, United States of America

[2]Center for Cancer Research and Therapeutic Development, Clark Atlanta University, 223 James P. Brawley Drive S.W., P.O. Box 1872, Atlanta, Georgia 30314, United States of America

Abstract

Background—Bone marrow stromal cell (BMSC) paracrine factor(s) can induce apoptosis in bone metastatic prostate cancer (PCa) cell lines. However, the PCa cells that escape BMSC-induced apoptosis can upregulate cytoprotective autophagy.

Methods—C4-2, C4-2B, MDA PCa 2a, MDA PCa 2b, VCaP, PC3, or DU145 PCa cell lines were grown in BMSC conditioned medium and analyzed for mRNA and/or protein accumulation of p62 (also known as Sequestome-1/SQSTM1), Microtubule-associated Protein 1 Light Chain 3B (LC3B), or Lysosomal-associated Membrane Protein 1 (LAMP1) using quantitative polymerase chain reaction (QPCR), western blot, or immunofluorescence. Small interfering RNA (siRNA) was used to determine if p62 is necessary PCa cell survival.

Results—BMSC paracrine signaling upregulated *p62* mRNA and protein in a subset of the PCa cell lines. The PCa cell lines that were insensitive to BMSC-induced apoptosis and autophagy induction had elevated basal *p62* mRNA and protein. In the BMSC-insensitive PCa cell lines, siRNA knockdown of *p62* was cytotoxic and immunostaining showed peri-nuclear clustering of autolysosomes. However, in the BMSC-sensitive PCa cell lines, *p62* siRNA knockdown was not appreciably cytotoxic and did not affect autolysosome subcellular localization.

Conclusions—A pattern emerges wherein the BMSC-sensitive PCa cell lines are known to be osteoblastic and express the androgen receptor, while the BMSC-insensitive PCa cell lines are characteristically osteolytic and do not express the androgen receptor. Furthermore, BMSC-insensitive PCa may have evolved a dependency on p62 for cell survival that could be exploited to target and kill these apoptosis-resistant PCa cells in the bone.

Keywords

p62/SQSTM1; autophagy; prostate cancer; bone paracrine factors; bone marrow

Introduction

To maintain homeostasis, cells can utilize autophagy to clear, degrade, and recycle cytoplasmic biomolecules (1,2). During autophagy, cytoplasmic contents are enveloped into

Corresponding Author: Nikki A. Delk, PhD, Address: Department of Biochemistry and Cell Biology, Rice University, BioScience Research Collaborative, 6500 Main, MS 601, Houston, TX 77030, United States of America, Phone: 713-348-8302, Fax: 713-348-5154, nadelk@rice.edu.

Disclosure Statement: No author on this manuscript has any conflict of interest to disclose regarding the work in this manuscript.

a double membrane vesicle called the autophagosome. The autophagosome fuses with the lysosome, forming the autolysosome, wherein hydrolases degrade the vesicle cargo. The degraded products are transported back into the cytoplasm for reuse by the cell (1,2). Microtubule-associated Protein 1 Light Chain 3 (LC3) is an autophagosome membrane protein that commonly serves as an autophagy induction and flux marker (3). When autophagy is induced, free cytoplasmic LC3 (LC3-I) is conjugated to phosphatidylethanolamine to form membrane-bound LC3 (LC3-II) (4). LC3-II is located on the outer and inner autophagosome double membrane (5). During autophagic flux, outer LC3-II is proteolytically cleaved from the membrane to replenish free LC3 and inner membrane LC3-II is degraded in the autolysosome (3,6,7).

The selective engulfment of cytoplasmic contents into autophagosomes requires auxiliary proteins, such as p62 (also known as Sequestome-1/SQSTM1) (2,8), a multifunctional, multi-domain scaffolding protein that serves as a hub for several signaling pathways, including autophagy-mediated protein degradation, Nuclear Factor Kappa-B (NF-κB) activation, and Nuclear Factor Erythroid 2-Related Factor 2 (NRF2) activation (8,9). In autophagy, p62 sequesters K63-linked polyubiquitinated proteins into the autophagosome through its ubiquitin-association (UBA) and LC3-interacting (LIR) domains (8,10-12). As a consequence, p62 also is degraded in the autolysosome (10,11). In transgenic mice or human specimens, p62 overaccumulation is associated with degenerative diseases, including neurodegeneration (13), liver cirrhosis (14-16), and cardiac myopathy (17). p62 overaccumulation can also promote tumor cell survival. Although the mechanisms of p62 function in the different pathologies remain unclear, possible mechanisms of p62-mediated tumorigenesis involve genetic instability, NF-κB-mediated inflammatory response, or NRF2-mediated antioxidant signaling. For example, p62 overexpression in autophagy-deficient cells leads to genetic instability and increases tumorigenesis in mouse allografts (18). In addition, in K-ras driven lung (19) and pancreatic (20) tumors, p62 is elevated and contributes to constitutive NF-κB activation by binding to and activating TNF receptor-associated factor 6 (TRAF6). Furthermore, in liver cancer, overaccumulated p62 binds to Kelch-Like ECH-Associated Protein (KEAP1), disrupting KEAP1-NFR2 interaction and allowing NRF2 transactivation of antioxidant and detoxifying genes (21). Notably, knockdown of p62 in mice reduces tumor growth (19,22). Indeed, p62 was found to be elevated in prostate (23), breast (24-26), pancreatic (20), lung (19,27), and liver (21) cancers.

Over 80% of PCa mortality is attributed to bone metastasis (28) and, thus, it is crucial to understand the molecular mechanisms that enable PCa survival in the bone. Through this study, we uncovered the effect of bone marrow stromal cell (BMSC) paracrine factors on *p62* mRNA expression and protein accumulation in bone metastatic PCa cells. Furthermore, we discovered that subtypes of PCa cell lines show differential autophagy induction, p62 accumulation, and p62-mediated cell survival in response to BMSC paracrine signaling. We conclude that paracrine factors in the bone microenvironment contribute to PCa cell survival and adaptation in the bone through a mechanism involving p62 regulation and propose that p62 may be a valuable biomarker and rational target for apoptosis-resistant bone metastatic PCa cells.

Materials and Methods

Cell Culture

PCa cell lines (C4-2, C4-2B, DU145, MDA PCa 2a, MDA PCa 2b, PC3, VCaP) and bone marrow stromal cell lines (HS-5, HS-27a) were grown in a 37°C, 5.0% (v/v) CO_2 growth chamber. C4-2, C4-2B, DU145, and PC3 cell lines were cultured in T-medium (Gibco/Invitrogen) supplemented with 5% (v/v) fetal bovine serum (FBS) (Atlanta Biologicals), 0.4

mM L-glutamine (L-glut) (Gibco/Invitrogen), and 10 U/ml penicillin G sodium and 10 mg/ml streptomycin sulfate (pen-strep) (Gibco/Invitrogen). MDA PCa 2a and MDA PCa 2b were cultured in BRFF-HPC1 medium (AthenaES; 0403) supplemented with 20% (v/v) FBS, 0.4 mM L-glut, and pen-strep. VCaP, HS-5, and HS-27a cell lines were cultured in low glucose DMEM medium (Gibco/Invitrogen) supplemented with 10% FBS, 0.4 mM L-glut, and pen-strep.

Conditioned Medium Treatment

To obtain bone marrow stromal cell conditioned medium, culture medium was removed from HS-5 or HS-27a cultured cells and replaced with fresh T-medium supplemented with 5% FBS, L-glut, pen-strep. After 3 days incubation, the conditioned T-medium was collected and spun at 1400 rpm for 3 minutes to remove cell debris. The conditioned media were stored at -80°C. T-medium supplemented with 5% FBS, L-glut, pen-strep served as the control growth medium.

Drug and siRNA Treatments

Cells were treated with chloroquine diphosphate aqueous solution (Invitrogen; P36235). Cells were transfected with a pool of three unique 27-mer *p62/SQSTM1* siRNA duplexes (Origene; SR305865) using siTran 1.0 transfection reagent (Origene; TT300001). Western blot analysis and/or immunostaining were used to confirm loss of p62 protein.

Western Blot Analysis and Antibodies

Protein was isolated from cells using NP40 lysis buffer (0.5% NP-40 (Sigma; NP40S), 50 mM Tris (pH 7.5), 150 mM NaCl, 3 mM MgCl2, 1× protease inhibitors (Roche; 0505489001). Protein concentration was measured using the Pierce BCA Protein Assay Kit (Thermo Scientific; 23225). For western blot analysis, equal protein concentrations were loaded onto and separated in 17% (w/v) sodium dodecyl sulfate polyacrylamide gel (40% acrylamide/bis-acrylamide solution; Bio-Rad; 161-0148). Proteins were transferred from the gel to 0.45 μm pore size nitrocellulose membrane (Bio-Rad; 162-0094) and total protein visualized using Ponceau S (Sigma; P7170). The membrane was blocked with 3% (w/v) bovine serum albumin (BSA) (Sigma-Aldrich; A7906) in 1× TBST (20 mM Tris, pH 7.6, 150 mM NaCl, 0.05% Tween-20). Primary and secondary antibodies were diluted in 3% BSA/1× TBST. Protein blot bands were visualized using Pierce ECL Western Blotting Substrate (Thermo Scientific; 32106) and imaged using the Fujifilm LAS-4000 imager (Fuji). *Densitometry:* Densitometry of western blot bands was performed using Image J software (http://rsbweb.nih.gov/ij/). To determine relative protein levels across treatments and/or cell lines, densitometric values for LC3B or p62 were first normalized to β-actin or Ponceau S stain loading controls and then normalized to a control treatment (set at 1.0). When comparing across cell lines, total protein (i.e. Ponceau S stain) was used as the loading control. *Primary antibodies:* LC3B (Novus Biologicals; NB600-1384), p62/SQSTM1 (Abnova; H00008878-M01), β-actin (Abcam; ab8226). *Secondary antibodies:* sheep anti-mouse (Jackson ImmunoResearch Laboratories; 515-035-062), goat anti-rabbit (Sigma-Aldrich; A6154).

RNA Extraction and Quantitative Polymerase Chain Reaction (QPCR)

To examine mRNA expression, cells were washed twice with 1× PBS and total RNA was extracted from the cells using Trizol reagent according to the manufacturer's instructions (Invitrogen; 15596-026) RNA was DNAse-treated (Ambion; AM1906) for 30 minutes at 37°C and, following, cDNA was made using Quanta Biosciences qScript cDNA Super mix (VWR; 95048). The QPCR reaction was prepared using Quanta Bioscience SYBR Green Super mix (VWR; 95030-214). Primers specific for *p62* were used and data was normalized

to the *β-actin* transcript levels. Relative mRNA levels were calculated using the $2^{-\Delta\Delta CT}$ method. *p62 primers:* Forward: AAA TGG GTC CAC CAG GAA ACT GGA; Reverse: TCA ACT TCA ATG CCC AGA GGG CTA. *β-actin primers:* Forward: GAT GAG ATT GGC ATG GCT TT; Reverse: CAC CTT CAC CGG TCC AGT TT.

Cell Viability

Calcein AM and ethidium homodimer 1 (EthD-1) fluorescent probes were used to stain live and dead cells, respectively, according to manufacturer's instructions (Molecular Probes; L3224). Briefly, 2 μM calcein AM and 4 μM EthD-1 were added directly to cells in culture. Following incubation, the cells were trypsinized and transferred to a 96-well tissue culture plate. Cell fluorescence was measured using the Infinite® M200 microplate reader (Tecan). Fluorescent cells also were imaged in the 96-well plate at 4× magnification (sufficient to capture 10,000 cells in a microscopy field) and counted by using Image J software (http://rsbweb.nih.gov/ij/). Cell viability was determined using the calculation live cells/(live + dead cells).

Immunofluorescence

Cells were fixed and permeabilized with 100% methanol at -20°C for at least 30 minutes. Cells were blocked with 2.5% BSA in 1× phosphate buffered saline (PBS) at room temperature for at least 30 minutes. Antibodies were diluted in 2.5% BSA in 1× PBS. Cells were incubated in primary antibody at 4°C overnight, washed with 1× PBS, and then incubated in fluorescently labeled secondary antibody at 4°C in the dark, overnight. *Primary antibodies:* LC3B (Novus Biologicals; NB600-1384), p62/SQSTM1 (Abnova; H00008878-M01), LAMP1 (University of Iowa Developmental Studies Hybridoma Bank; H4A3). *Fluorescently labeled secondary antibodies:* Alexafluor 488, goat anti-mouse (Invitrogen; A11001), Alexafluor 568, goat anti-rabbit (Invitrogen; A11061).

Microscopy

Images were taken and processed using the Eclipse TE300 inverted microscope (Nikon) and NIS Elements software (Nikon) (40× magnification, scale bar = 100 μm). Alexafluor 488 and 568 fluorescence was detected using the FITC and Texas Red filters, respectively.

Statistics

Statistical significance was determined using unpaired student t test.

Results

HS-5 paracrine factor(s) can induce PCa autophagy

We previously reported that the hematopoietic HS-5 bone marrow stromal cell line, but not the HS-27a structural bone marrow stromal cell line, secretes a milieu of soluble factor(s) that induce LC3B-II protein accumulation in C4-2 and C4-2B bone metastatic PCa cell lines (29). We expanded our analysis to determine if LC3B-II upregulation is a common response of bone metastatic PCa cell lines (Table I, (30-42)) to HS-5 secreted factor(s). Thus, we grew MDA PCa 2a, MDA PCa 2b and VCaP PCa cell lines for several days in control growth medium or in HS-5 or HS-27a bone marrow stromal cell (BMSC) conditioned medium and used western blot analysis to determine LC3B-II protein levels. As previously observed for the C4-2 and C4-2B cell lines (29), HS-5 conditioned medium induced greater LC3B-II accumulation in MDA PCa 2a, MDA PCa 2b and VCaP cells than did control growth medium or HS-27a BMSC conditioned medium (Fig. 1A).

LC3B-II accumulation can indicate autophagy induction or, alternatively, inhibition of autophagic flux (3). Using the lysomotropic inhibitor, chloroquine, we previously showed that autophagic flux is maintained in C4-2 and C4-2B cells in the presence of HS-5 conditioned medium (29). To further confirm that autophagic flux remains functional in PCa cells grown in HS-5 conditioned medium, we also treated MDA PCa 2a and MDA PCa 2b cell lines with 40 μM chloroquine in the presence of HS-5 BMSC conditioned medium for two days. As observed for C4-2 and C4-2B cell lines (Fig. 1B, (29)), chloroquine increased LC3B-II accumulation over the vehicle control in MDA PCa 2a and MDA PCa 2b cells (Fig. 1B). Thus, HS-5 BMSC paracrine factor(s) do not inhibit autophagic flux in the bone metastatic PCa cell lines analyzed, but rather, induce PCa cell autophagy.

HS-5 paracrine factor(s) can upregulate PCa *p62* mRNA and protein

While characterizing HS-5-induced autophagy response in C4-2, C4-2B, MDA PCa 2a, MDA PCa 2b, and VCaP cell lines, we discovered a steady-state increase in p62 protein that occurred within one day of growth in HS-5 BMSC conditioned medium (Fig. 1A). For example, HS5 conditioned medium induced a 1.7- to 4.2-fold increase in p62 protein over control medium (Fig. 1A). Because p62 sequesters ubiquitinated proteins into the autophagosome for degradation, it also is degraded through autophagy (10,11). Therefore, our results were unexpected given that HS-5 conditioned medium induces autophagy and does not block autophagy flux in PCa cells (Fig. 1, (29)). Furthermore, chloroquine increased p62 protein in the PCa cell lines grown in control medium or HS-5 or HS-27a BMSC conditioned medium (Fig. 1B), indicating that p62 is properly degraded through autophagy under these growth conditions. Therefore we investigated the effect of HS-5 conditioned medium on *p62* mRNA levels in the PCa cell lines. Quantitative polymerase chain reaction (QPCR) revealed that within one day, HS-5 conditioned medium upregulated *p62* mRNA levels (Fig. 1C). Thus, our results suggest (post)transcriptional regulation of PCa *p62* by HS-5-secreted factor(s) and likely do not indicate a defect in autophagic flux.

DU145 and PC3 cell lines show no significant autophagy or *p62* induction when exposed to HS-5 paracrine factor(s)

HS-5 BMSC conditioned medium induces apoptosis in C4-2, C4-2B, and VCaP cells (data not shown, (43)). Autophagy, which we propose is cytoprotective in this context, is induced in the surviving subpopulation ((29), data not shown). The DU145 and PC3 bone metastatic PCa cell lines are less sensitive to HS-5-induced apoptosis (43). Therefore, we predicted that DU145 and PC3 cells can escape HS-5-induced apoptosis by upregulating cytoprotective autophagy more efficiently than the apoptosis-sensitive PCa cell lines. To test our hypothesis, we compared the HS-5-mediated autophagy response of the DU145 and PC3 cells with that of the C4-2 cell line. C4-2, DU145, and PC3 cells were grown in control or BMSC conditioned medium for two days and analyzed for LC3B protein accumulation. Relative to control growth medium or HS-27a BMSC conditioned medium, HS-5 BMSC conditioned medium led to a greater induction of LC3B-I and/or LC3B-II accumulation in C4-2 cells than in DU145 or PC3 cells (Fig. 2A). For example, relative to control growth medium, HS-5 conditioned medium increased LC3B-I and LC3B-II levels 4.1- and 5-fold, respectively, in C4-2 cells, but had comparatively less effect on LC3B-I or LC3B-II protein levels in PC3 cells (Fig. 2A). Furthermore, while DU145 cells showed an increase in LC3-I when grown in HS-5 conditioned medium over control growth medium, we could not detect LC3B-II by western blot (Fig. 2A). Thus, HS-5 paracrine factor(s) have a more profound effect on autophagy induction in C4-2 cells than in DU145 or PC3 cells.

Because we found that DU145 cells do not accumulate LC3B-II when grown in control growth medium or BMSC conditioned medium (Fig. 2A), we concluded that canonical autophagy is not the common mechanism that mediates survival of DU145 and PC3 cells

exposed to HS-5 paracrine factor(s). However, p62 also promotes cell survival both dependently and independently of autophagy (9) and is induced by HS-5 conditioned medium in multiple PCa cell lines (Fig. 1A). Therefore, we compared the effect of HS-5 BMSC conditioned medium on *p62* mRNA and protein accumulation in C4-2, DU145 and PC3 cell lines. Relative to control growth medium, after two days growth in HS-5 conditioned medium, C4-2 cells showed a 3.9- and 2.5-fold increase in *p62* mRNA and protein, respectively (Fig. 2A & B). However, DU145 and PC3 cells showed no considerable increase in *p62* mRNA or protein accumulation when grown in HS-5 conditioned medium (Fig. 2A & B). Taken together, our data reveal that, unlike the C4-2, C4-2B, MDA PCa 2a, MDA PCa 2b, or VCaP cell lines, the DU145 and PC3 cell lines show no notable autophagy or *p62* induction in response to HS5-secreted paracrine factor(s).

DU145 and PC3 cell lines have high basal *p62* levels

While we did not detect a considerable effect of HS-5 conditioned medium on autophagy induction or *p62* mRNA and protein accumulation in DU145 or PC3 cell lines (Fig. 2A & B), we did observe that DU145 and PC3 cells have comparatively higher basal *p62* mRNA and/or protein levels than the C4-2, C4-2B, MDA PCa 2a, MDA PCa 2b, or VCaP cell lines (Fig. 2A, B, & C). For example, when normalized to C4-2 basal *p62* mRNA (Fig. 2B) or protein (Fig. 2A), *p62* mRNA or protein levels were 11- or 5.5-fold and 2.8- or 3.4-fold greater in DU145 and PC3 cells, respectively.

Down regulation of *p62* is cytotoxic for DU145 and PC3 cell lines

Given that both DU145 and PC3 cell lines have reduced sensitivity to HS-5-induced apoptosis (43) and show comparatively high basal *p62* mRNA and protein levels (Fig. 2), we explored the possible role of p62 in DU145 and PC3 cell survival. C4-2, DU145 and PC3 cells were grown in control growth medium and transiently transfected with 40 nM *p62* siRNA to reduce p62 protein accumulation (Fig. 3A). Three days following treatment, cells were analyzed for the presence of live and dead cells by measuring calcein AM and ethidium homodimer 1 (EthD-1) fluorescence, respectively (graph not shown). Relative to control siRNA, down regulation of *p62* significantly reduced the calcein AM fluorescence (p-value = 0.003) and increased EthD-1 fluorescence (p-value = 0.014) in PC3 cells. Thus, p62 mediates PC3 cell survival. However, *p62* siRNA did not significantly affect calcein AM (p-value = 0.29) or EthD-1 (p-value = 0.31) fluorescence in C4-2 cells, implying that p62 is not necessary for C4-2 cell survival in normal under control growth conditions.

In our experiments, 40 nM *p62* siRNA was relatively less effective at reducing p62 protein accumulation in DU145 cells (Fig. 3A) and did not have an effect on DU145 cell survival (calcein AM, p-value = 0.49; EthD-1, p-value = 0.17; graph not shown). However, transient transfection of 60 nM *p62* siRNA was sufficient to reduce p62 protein accumulation to nearly undetectable levels in DU145 cells (Fig. 3A). Therefore, we transfected C4-2, C4-2B, MDA PCa 2A, MDA PCa 2B, DU145, and PC3 cells grown in control growth medium with 60 nM *p62* siRNA and after two days we measured cell viability by counting calcein AM and EthD-1 fluorescent cells. In control growth media, down regulation of p62 protein significantly reduced the cell viability of DU145 (p-value ≤ 0.0005) and PC3 (p-value ≤ 0.0005) cells, but had less effect on C4-2 (p-value ≤ 0.05), C4-2B, MDA PCa 2a, or MDA PCa 2b cell viability (Fig. 3B, Supplemental Fig. 1).

When p62 protein was reduced under control growth conditions, C4-2, C4-2B, MDA PCa 2a, and MDA PCa 2b cells did not show as significant of a reduction in cell viability as the DU145 or PC3 cells (Fig. 3B, Supplemental Fig. 1). However, given that HS-5 BMSC conditioned medium upregulated *p62* mRNA and protein in C4-2, C4-2B, MDA PCa 2a, and MDA PCa 2b cells (Fig. 1 & 2), we reasoned that p62 may have a cytoprotective

function in the presence of HS5 conditioned medium. Surprisingly, siRNA-mediated knockdown of *p62* did not reduce the cell viability of C4-2 or C4-2B cells grown in HS-5 conditioned medium (Fig. 3B). However, transient transfection of 60 nM *p62* siRNA into DU145 and PC3 cells grown in HS-5 conditioned medium for two days significantly reduced the cell viability (DU145, p-value ≤ 0.0005 ; PC3, p-value ≤ 0.005) (Fig. 3B). Interestingly, we were unable to appreciably reduce p62 protein levels using siRNA in MDA PCa 2a or MDA PCa 2b cells grown in HS-5 conditioned medium (Supplemental Fig. 1). Taken together, these data demonstrate that that loss of p62 protein is more significantly cytotoxic for DU145 and PC3 cells than for C4-2, C4-2B, MDA PCa 2a, or MDA PCa 2b cell lines grown in control or HS-5 BMSC conditioned growth media.

Down regulation of *p62* alters autolysosomal subcellular localization in DU145 and PC3 cell lines

To investigate the effect of the loss of p62 protein on autolysosome accumulation in individual cells, we performed co-immunostaining for LC3B and p62 or the lysosomal membrane protein, LAMP1, in C4-2, C4-2B, DU145, and PC3 cells transiently transfected with 60 nM *p62* siRNA and grown in control growth medium or HS-5 BMSC conditioned medium for two days. In C4-2 and C4-2B cells grown in control growth medium or HS-5 conditioned medium, discrete co-localized LC3B and LAMP1 structures (autolysosomes) were found distributed throughout the cytoplasm and around the nucleus in cells transfected with control siRNA or *p62* siRNA (Fig. 4A & B). However, in PC3 cells, the subcellular co-localization of LC3B and LAMP1 changed from cytoplasmic distribution to peri-nuclear clustering when p62 was down regulated (Fig. 4A & B, arrows). LC3B puncta did not accumulate in DU145 cells (data not shown), presumably because DU145 cells do not accumulate LC3B-II (Fig. 2A). However, as observed for PC3 cells, *p62* siRNA led to peri-nuclear clustering of LAMP1 in DU145 cells grown in control growth medium or HS-5 conditioned medium (Fig. 4A & B, arrows). Thus, the loss of p62 has a similar effect on lysosome and autolysosome subcellular localization in DU145 and PC3 cell lines in grown in either control growth medium or HS-5 BMSC conditioned medium, but *p62* siRNA does not affect autolysosome subcellular localization in C4-2 or C4-2B cells.

Discussion

Sensitivity to HS-5 secreted factors correlates with PCa androgen receptor expression and bone-forming tumor type

An intriguing similarity emerges for the PCa cell lines which we discovered can respond to HS-5 BMSC-induced apoptosis, autophagy, or p62 accumulation in contrast to the PCa cell lines that did not show a significant apoptosis, autophagy, or p62 induction response to HS-5 paracrine factor(s) (Fig. 5). The PCa cell lines (C4-2, C4-2B, MDA PCa 2a, MDA PCa 2b, and VCaP) that were sensitive to HS-5 conditioned medium express the androgen receptor (41) and form primarily osteoblastic lesions in mice (33,42,44), while the HS-5-insensitive PCa cells lines (DU145 and PC3) do not express the androgen receptor (41) and form primarily osteolytic lesions (37). It is feasible that the osteolytic PCa cell types either secrete factor(s) that neutralize the bone cell paracrine signals that induce apoptosis, autophagy, or p62 accumulation, or alternatively lack internal pathways that allow them to respond to these signals. Another possibility is that the androgen receptor can directly or indirectly mediate the induction of cytoprotective autophagy and p62 upregulation in PCa cells in response to BMSC-secreted apoptosis-inducing factor(s). Experiments are underway to determine the mechanistic role of the androgen receptor in HS-5-induced autophagy and p62 upregulation and to determine if key autophagy regulators are transcriptional targets of the androgen receptor.

p62 is required for the cell survival of HS-5-insensitive cell lines

If the androgen receptor indeed mediates autophagy induction in response to HS-5 BMSC paracrine factors, then not surprisingly, DU145 and PC3 PCa cells, which lack androgen receptor expression, were non-responsive to HS-5-induced autophagy. Interestingly, the PC3 cells accumulated more basal LC3B-II than did the HS-5-sensitive PCa cell lines (Fig. 2 & 3, data not shown), implying that high basal autophagy protects PC3 cells from HS-5-induced apoptosis. While PC3 cells may have higher basal autophagy, DU145 cells do not carry out canonical autophagy (45). For example, we did not detect LC3B-II (Fig. 2 & 3) or LC3B-decorated autophagosomes or autolysosomes (data not shown) in the DU145 cells. Furthermore, Ouyang and colleagues recently reported that ATG5, which promotes autophagosome formation, is mutated and non-functional in DU145 cells (45). Yet, both DU145 and PC3 cell lines are insensitive to HS-5-induced apoptosis (43), suggesting that these cell lines share an androgen receptor-independent – and possibly autophagy-independent – survival mechanism. Our data reveals that one such shared alternative cell survival mechanism requires p62 (Fig. 5). Because p62 is a multifunctional protein, there are several candidate cell survival pathways that may be compromised in DU145 and PC3 cells when *p62* expression is reduced. For example, in addition to mediating autophagic degradation of cytotoxic polyubiquitinated protein aggregates, p62 also promotes cell survival through NF-κB activation and NRF2 antioxidant signaling (8,9). It will be important to determine the regulation and activity of the various p62-mediated cell survival pathways when *p62* is knocked down in DU145 and PC3 PCa cell lines, as these pathways may serve as biomarkers or therapeutic targets.

PCa cell lines with high basal p62 may have evolved a cell survival requirement for p62

We initially predicted that the steady-state upregulation of *p62* mRNA and protein levels in HS-5-sensitive PCa cell lines exposed to HS-5 paracrine signaling reflected a cytoprotective response. However, in our experiments, p62 did not appear necessary for the survival of HS-5-sensitive PCa cell lines under normal growth conditions or in the presence of HS-5 paracrine factor(s) (Fig. 3, Supplemental Fig. 1, data not shown). Our results imply that under normal growth conditions or in the presence of HS-5 paracrine factors, the HS-5-sensitive PCa cell lines, which do not normally accumulate high levels of p62, have cell survival pathways that can compensate for the loss of p62.

In contrast, under normal growth conditions or in the presence of HS-5 BMSC paracrine factors DU145 and PC3 cells showed high basal levels of *p62* mRNA and protein and required p62 for cell survival (Fig. 2 & 3). Thus, we propose that the DU145 and PC3 PCa cell lines have evolved a cell survival dependency on p62 and that constitutive, long-term p62 elevation may be important for PCa adaptation to the bone microenvironment (Fig. 5).

Defective autophagy flux accounts for, in part, the high basal p62 protein accumulation in DU145 cells (45). However, we also saw an increase in basal *p62* mRNA levels in both the DU145 and PC3 cells (Fig. 2), suggesting enhanced transcriptional activity and/or mRNA stability. Furthermore, HS-5-induced p62 accumulation occurred at the level of mRNA in the HS-5-sensitive PCa cell lines (Fig. 2). Transcription factors and microRNAs shown to regulate *p62* expression or mRNA stability include NF-κB (20), NRF2 (46), Farnesoid Receptor X (47), Prostate Derived Ets Factor (26), or miR-17/20/93/106 (48)). One or more of these regulators of *p62* mRNA levels may mediate HS-5-induced *p62* expression in the HS-5-sensitive cell lines and these regulators may have altered activity in the DU145 and PC3 cell lines. Future investigation into the mechanistic regulation of *p62* expression in the PCa cells lines will provide strategies to target p62 function in cancer cells.

Autolysosome peri-nuclear clustering is associated with enhanced autophagy induction and flux

In DU145 and PC3 cells we observed that lysosomes and autolysosomes, respectively, are normally distributed throughout the cytoplasm and around the nucleus (Fig. 4). However, *p62* knockdown caused peri-nuclear clustering of (auto)lysosomes in DU145 and PC3 cells. Other laboratories have reported that autolysosome clustering is associated with enhanced autophagy induction and flux in response to viral infection (49) or hypertonic stress (50) . In accordance, we detected peri-nuclear clustering of (auto)lysosomes in DU145 and PC3 cells that had avoided *p62* siRNA-mediated cell death at the time of analysis and thus the (auto)lysosome peri-nuclear clustering could have indicated a cell survival response. Alternatively, *p62* siRNA induced (auto)lysosome clustering in DU145 and PC3 cells could be an indicator of impending cell death, as this altered subcellular localization of autolysosomes was not detected in C4-2 cells which are comparatively insensitive to *p62* siRNA-mediated cell death . The mechanism of the *p62*-siRNA-induced (auto)lysosome clustering is unclear, but likely involves regulation of trafficking along microtubules (49,50).

Conclusion

p62 may be a rational target for bone metastatic PCa

p62 is overexpressed in multiple cancer types, including PCa, and can correlate with disease progression (19-21,23-27). In line with these findings, our data suggests that the bone microenvironment can contribute to the upregulation of *p62* mRNA and protein in metastatic PCa cells and it will be important to determine *p62* expression in patient bone metastases. Notably, DU145 and PC3 cell lines represent a PCa cell subtype that would be resistant to androgen deprivation or anti-androgen therapies due to lack of androgen receptor expression. Importantly, our data suggest that treatment resistant PCa tumors could be identified by *p62* expression and subsequently killed by targeting *p62* expression and/or the function of p62 in one or more pathways, including autophagy, NF-κB activation, or NRF2 signaling. In line with our reasoning, knockdown of p62 accumulation in bone marrow stromal cells attenuated, among several signaling cascades, NF-κB signaling and cytokine secretion and concomitantly attenuated bone marrow stromal cell paracrine support of multiple myeloma cell proliferation (51). Thus, it is intriguing to speculate that targeting *p62* expression and/or function in bone metastatic PCa cells would not only lead to PCa cell death, but could disrupt potential p62-mediated, tumor-promoting cross talk between PCa and bone cells in the metastatic microenvironment.

Supplementary Material

Refer to Web version on PubMed Central for supplementary material.

Acknowledgments

We would like to thank all of the members of the labs of Drs. Mary C. Farach-Carson, Daniel Carson, Cimona V. Hinton, and Nora Navone and all of the members of the Prostate Cancer P01 group for scientific discussion and/or technical support. This work was supported by NIH Funding support from NIH/NCI K01 CA160602, NIH/NCI F32 CA128296, and NIH/NCI P01 CA098912.

References

1. Mizushima N. Autophagy: process and function. Genes Dev. 2007; 21(22):2861–2873. [PubMed: 18006683]

2. Rabinowitz JD, White E. Autophagy and metabolism. Science. 2010; 330(6009):1344–1348. [PubMed: 21127245]

3. Mizushima N, Yoshimori T. How to interpret LC3 immunoblotting. Autophagy. 2007; 3(6):542–545. [PubMed: 17611390]

4. Kabeya Y, Mizushima N, Yamamoto A, Oshitani-Okamoto S, Ohsumi Y, Yoshimori T. LC3, GABARAP and GATE16 localize to autophagosomal membrane depending on form-II formation. J Cell Sci. 2004; 117(Pt 13):2805–2812. [PubMed: 15169837]

5. Kabeya Y, Mizushima N, Ueno T, Yamamoto A, Kirisako T, Noda T, Kominami E, Ohsumi Y, Yoshimori T. LC3, a mammalian homologue of yeast Apg8p, is localized in autophagosome membranes after processing. EMBO J. 2000; 19(21):5720–5728. [PubMed: 11060023]

6. Satoo K, Noda NN, Kumeta H, Fujioka Y, Mizushima N, Ohsumi Y, Inagaki F. The structure of Atg4B-LC3 complex reveals the mechanism of LC3 processing and delipidation during autophagy. EMBO J. 2009; 28(9):1341–1350. [PubMed: 19322194]

7. Tanida I, Minematsu-Ikeguchi N, Ueno T, Kominami E. Lysosomal turnover, but not a cellular level, of endogenous LC3 is a marker for autophagy. Autophagy. 2005; 1(2):84–91. [PubMed: 16874052]

8. Komatsu M, Ichimura Y. Physiological significance of selective degradation of p62 by autophagy. FEBS Lett. 2010; 584(7):1374–1378. [PubMed: 20153326]

9. White E. Deconvoluting the context-dependent role for autophagy in cancer. Nat Rev Cancer. 2012; 12(6):401–410. [PubMed: 22534666]

10. Pankiv S, Clausen TH, Lamark T, Brech A, Bruun JA, Outzen H, Overvatn A, Bjorkoy G, Johansen T. p62/SQSTM1 binds directly to Atg8/LC3 to facilitate degradation of ubiquitinated protein aggregates by autophagy. J Biol Chem. 2007; 282(33):24131–24145. [PubMed: 17580304]

11. Shvets E, Fass E, Scherz-Shouval R, Elazar Z. The N-terminus and Phe52 residue of LC3 recruit p62/SQSTM1 into autophagosomes. J Cell Sci. 2008; 121(Pt 16):2685–2695. [PubMed: 18653543]

12. Wooten MW, Geetha T, Babu JR, Seibenhener ML, Peng J, Cox N, Diaz-Meco MT, Moscat J. Essential role of sequestosome 1/p62 in regulating accumulation of Lys63-ubiquitinated proteins. J Biol Chem. 2008; 283(11):6783–6789. [PubMed: 18174161]

13. Inoue K, Rispoli J, Kaphzan H, Klann E, Chen EI, Kim J, Komatsu M, Abeliovich A. Macroautophagy deficiency mediates age-dependent neurodegeneration through a phospho-tau pathway. Mol Neurodegener. 2012; 7:48. [PubMed: 22998728]

14. Komatsu M, Kurokawa H, Waguri S, Taguchi K, Kobayashi A, Ichimura Y, Sou YS, Ueno I, Sakamoto A, Tong KI, Kim M, Nishito Y, Iemura S, Natsume T, Ueno T, Kominami E, Motohashi H, Tanaka K, Yamamoto M. The selective autophagy substrate p62 activates the stress responsive transcription factor Nrf2 through inactivation of Keap1. Nat Cell Biol. 2010; 12(3):213–223. [PubMed: 20173742]

15. Sasaki M, Miyakoshi M, Sato Y, Nakanuma Y. A possible involvement of p62/sequestosome-1 in the process of biliary epithelial autophagy and senescence in primary biliary cirrhosis. Liver Int. 2011; 32(3):487–499. [PubMed: 22098537]

16. Taguchi K, Fujikawa N, Komatsu M, Ishii T, Unno M, Akaike T, Motohashi H, Yamamoto M. Keap1 degradation by autophagy for the maintenance of redox homeostasis. Proc Natl Acad Sci U S A. 2012; 109(34):13561–13566. [PubMed: 22872865]

17. Hua Y, Zhang Y, Ceylan-Isik AF, Wold LE, Nunn JM, Ren J. Chronic Akt activation accentuates aging-induced cardiac hypertrophy and myocardial contractile dysfunction: role of autophagy. Basic Res Cardiol. 2011; 106(6):1173–1191. [PubMed: 21901288]

18. Mathew R, Karp CM, Beaudoin B, Vuong N, Chen G, Chen HY, Bray K, Reddy A, Bhanot G, Gelinas C, Dipaola RS, Karantza-Wadsworth V, White E. Autophagy suppresses tumorigenesis through elimination of p62. Cell. 2009; 137(6):1062–1075. [PubMed: 19524509]

19. Duran A, Linares JF, Galvez AS, Wikenheiser K, Flores JM, Diaz-Meco MT, Moscat J. The signaling adaptor p62 is an important NF-kappaB mediator in tumorigenesis. Cancer Cell. 2008; 13(4):343–354. [PubMed: 18394557]

20. Ling J, Kang Y, Zhao R, Xia Q, Lee DF, Chang Z, Li J, Peng B, Fleming JB, Wang H, Liu J, Lemischka IR, Hung MC, Chiao PJ. KrasG12D-induced IKK2/beta/NF-kappaB activation by

IL-1alpha and p62 feedforward loops is required for development of pancreatic ductal adenocarcinoma. Cancer Cell. 2012; 21(1):105–120. [PubMed: 22264792]

21. Inami Y, Waguri S, Sakamoto A, Kouno T, Nakada K, Hino O, Watanabe S, Ando J, Iwadate M, Yamamoto M, Lee MS, Tanaka K, Komatsu M. Persistent activation of Nrf2 through p62 in hepatocellular carcinoma cells. J Cell Biol. 2011; 193(2):275–284. [PubMed: 21482715]
22. Takamura A, Komatsu M, Hara T, Sakamoto A, Kishi C, Waguri S, Eishi Y, Hino O, Tanaka K, Mizushima N. Autophagy-deficient mice develop multiple liver tumors. Genes Dev. 2011; 25(8): 795–800. [PubMed: 21498569]
23. Kitamura H, Torigoe T, Asanuma H, Hisasue SI, Suzuki K, Tsukamoto T, Satoh M, Sato N. Cytosolic overexpression of p62 sequestosome 1 in neoplastic prostate tissue. Histopathology. 2006; 48(2):157–161. [PubMed: 16405664]
24. Choi J, Jung W, Koo JS. Expression of autophagy-related markers beclin-1, light chain 3A, light chain 3B and p62 according to the molecular subtype of breast cancer. Histopathology. 2012; 62(2):275–286. [PubMed: 23134379]
25. Rolland P, Madjd Z, Durrant L, Ellis IO, Layfield R, Spendlove I. The ubiquitin-binding protein p62 is expressed in breast cancers showing features of aggressive disease. Endocr Relat Cancer. 2007; 14(1):73–80. [PubMed: 17395976]
26. Thompson HG, Harris JW, Wold BJ, Lin F, Brody JP. p62 overexpression in breast tumors and regulation by prostate-derived Ets factor in breast cancer cells. Oncogene. 2003; 22(15):2322–2333. [PubMed: 12700667]
27. Inoue D, Suzuki T, Mitsuishi Y, Miki Y, Suzuki S, Sugawara S, Watanabe M, Sakurada A, Endo C, Uruno A, Sasano H, Nakagawa T, Satoh K, Tanaka N, Kubo H, Motohashi H, Yamamoto M. Accumulation of p62/SQSTM1 is associated with poor prognosis in patients with lung adenocarcinoma. Cancer Sci. 2012; 103(4):760–766. [PubMed: 22320446]
28. Bubendorf L, Schopfer A, Wagner U, Sauter G, Moch H, Willi N, Gasser TC, Mihatsch MJ. Metastatic patterns of prostate cancer: an autopsy study of 1,589 patients. Hum Pathol. 2000; 31(5):578–583. [PubMed: 10836297]
29. Delk NA, Farach-Carson MC. Interleukin-6: a bone marrow stromal cell paracrine signal that induces neuroendocrine differentiation and modulates autophagy in bone metastatic PCa cells. Autophagy. 2012; 8(4):650–663. [PubMed: 22441019]
30. Chlenski A, Nakashiro K, Ketels KV, Korovaitseva GI, Oyasu R. Androgen receptor expression in androgen-independent prostate cancer cell lines. Prostate. 2001; 47(1):66–75. [PubMed: 11304731]
31. Horoszewicz JS, Leong SS, Chu TM, Wajsman ZL, Friedman M, Papsidero L, Kim U, Chai LS, Kakati S, Arya SK, Sandberg AA. The LNCaP cell line--a new model for studies on human prostatic carcinoma. Prog Clin Biol Res. 1980; 37:115–132. [PubMed: 7384082]
32. Kaighn ME, Lechner JF, Narayan KS, Jones LW. Prostate carcinoma: tissue culture cell lines. Natl Cancer Inst Monogr. 1978; (49):17–21. [PubMed: 571045]
33. Kirschenbaum A, Liu XH, Yao S, Leiter A, Levine AC. Prostatic acid phosphatase is expressed in human prostate cancer bone metastases and promotes osteoblast differentiation. Ann N Y Acad Sci. 2011; 1237:64–70. [PubMed: 22082367]
34. Korenchuk S, Lehr JE, L MC, Lee YG, Whitney S, Vessella R, Lin DL, Pienta KJ. VCaP, a cell-based model system of human prostate cancer. In Vivo. 2001; 15(2):163–168. [PubMed: 11317522]
35. Lin DL, Tarnowski CP, Zhang J, Dai J, Rohn E, Patel AH, Morris MD, Keller ET. Bone metastatic LNCaP-derivative C4-2B prostate cancer cell line mineralizes in vitro. Prostate. 2001; 47(3):212–221. [PubMed: 11351351]
36. Navone NM, Olive M, Ozen M, Davis R, Troncoso P, Tu SM, Johnston D, Pollack A, Pathak S, von Eschenbach AC, Logothetis CJ. Establishment of two human prostate cancer cell lines derived from a single bone metastasis. Clin Cancer Res. 1997; 3(12 Pt 1):2493–2500. [PubMed: 9815652]
37. Nemeth JA, Harb JF, Barroso U Jr, He Z, Grignon DJ, Cher ML. Severe combined immunodeficient-hu model of human prostate cancer metastasis to human bone. Cancer Res. 1999; 59(8):1987–1993. [PubMed: 10213511]

38. Roecklein BA, Torok-Storb B. Functionally distinct human marrow stromal cell lines immortalized by transduction with the human papilloma virus E6/E7 genes. Blood. 1995; 85(4):997–1005. [PubMed: 7849321]
39. Stone KR, Mickey DD, Wunderli H, Mickey GH, Paulson DF. Isolation of a human prostate carcinoma cell line (DU 145). Int J Cancer. 1978; 21(3):274–281. [PubMed: 631930]
40. Thalmann GN, Anezinis PE, Chang SM, Zhau HE, Kim EE, Hopwood VL, Pathak S, von Eschenbach AC, Chung LW. Androgen-independent cancer progression and bone metastasis in the LNCaP model of human prostate cancer. Cancer Res. 1994; 54(10):2577–2581. [PubMed: 8168083]
41. van Bokhoven A, Varella-Garcia M, Korch C, Johannes WU, Smith EE, Miller HL, Nordeen SK, Miller GJ, Lucia MS. Molecular characterization of human prostate carcinoma cell lines. Prostate. 2003; 57(3):205–225. [PubMed: 14518029]
42. Yang J, Fizazi K, Peleg S, Sikes CR, Raymond AK, Jamal N, Hu M, Olive M, Martinez LA, Wood CG, Logothetis CJ, Karsenty G, Navone NM. Prostate cancer cells induce osteoblast differentiation through a Cbfa1-dependent pathway. Cancer Res. 2001; 61(14):5652–5659. [PubMed: 11454720]
43. Zhang C, Soori M, Miles FL, Sikes RA, Carson DD, Chung LW, Farach-Carson MC. Paracrine factors produced by bone marrow stromal cells induce apoptosis and neuroendocrine differentiation in prostate cancer cells. Prostate. 2010; 71(2):157–167. [PubMed: 20665531]
44. Wu TT, Sikes RA, Cui Q, Thalmann GN, Kao C, Murphy CF, Yang H, Zhau HE, Balian G, Chung LW. Establishing human prostate cancer cell xenografts in bone: induction of osteoblastic reaction by prostate-specific antigen-producing tumors in athymic and SCID/bg mice using LNCaP and lineage-derived metastatic sublines. Int J Cancer. 1998; 77(6):887–894. [PubMed: 9714059]
45. Ouyang DY, Xu LH, He XH, Zhang YT, Zeng LH, Cai JY, Ren S. Autophagy is differentially induced in prostate cancer LNCaP, DU145 and PC-3 cells via distinct splicing profiles of ATG5. Autophagy. 2012; 9(1):20–32. [PubMed: 23075929]
46. Jain A, Lamark T, Sjottem E, Larsen KB, Awuh JA, Overvatn A, McMahon M, Hayes JD, Johansen T. p62/SQSTM1 is a target gene for transcription factor NRF2 and creates a positive feedback loop by inducing antioxidant response element-driven gene transcription. J Biol Chem. 2010; 285(29):22576–22591. [PubMed: 20452972]
47. Williams JA, Thomas AM, Li G, Kong B, Zhan L, Inaba Y, Xie W, Ding WX, Guo GL. Tissue specific induction of p62/Sqstm1 by farnesoid X receptor. PLoS One. 2012; 7(8):e43961. [PubMed: 22952826]
48. Meenhuis A, van Veelen PA, de Looper H, van Boxtel N, van den Berge IJ, Sun SM, Taskesen E, Stern P, de Ru AH, van Adrichem AJ, Demmers J, Jongen-Lavrencic M, Lowenberg B, Touw IP, Sharp PA, Erkeland SJ. MiR-17/20/93/106 promote hematopoietic cell expansion by targeting sequestosome 1-regulated pathways in mice. Blood. 118(4):916–925. [PubMed: 21628417]
49. Berryman S, Brooks E, Burman A, Hawes P, Roberts R, Netherton C, Monaghan P, Whelband M, Cottam E, Elazar Z, Jackson T, Wileman T. Foot-and-mouth disease virus induces autophagosomes during cell entry via a class III phosphatidylinositol 3-kinase-independent pathway. J Virol. 2012; 86(23):12940–12953. [PubMed: 22993157]
50. Nunes P, Ernandez T, Roth I, Qiao X, Strebel D, Bouley R, Charollais A, Ramadori P, Foti M, Meda P, Feraille E, Brown D, Hasler U. Hypertonic stress promotes autophagy and microtubule-dependent autophagosomal clusters. Autophagy. 2013; 9(4):550–567. [PubMed: 23380587]
51. Hiruma Y, Honjo T, Jelinek DF, Windle JJ, Shin J, Roodman GD, Kurihara N. Increased signaling through p62 in the marrow microenvironment increases myeloma cell growth and osteoclast formation. Blood. 2009; 113(20):4894–4902. [PubMed: 19282458]

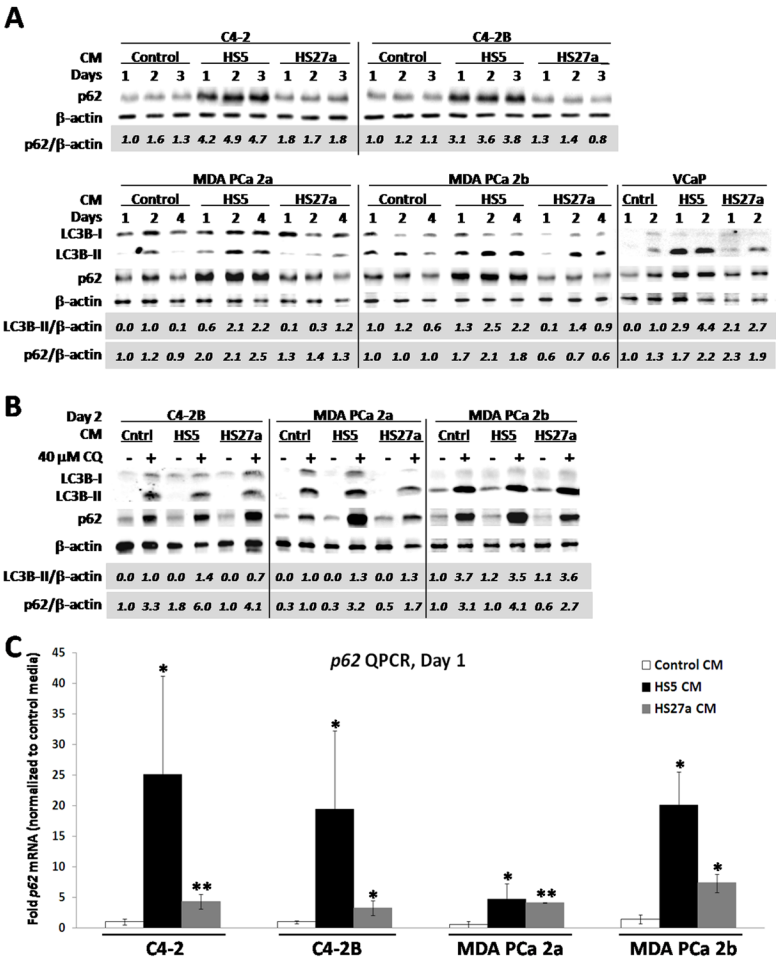

Figure 1. HS-5 BMSC paracrine factor(s) can induce autophagy and *p62* mRNA and protein accumulation in PCa cell lines

(A) MDA PCa 2a, MDA PCa 2b, and VCaP PCa cell lines were grown in control growth medium or in conditioned medium (CM) from HS-5 or HS-27a BMSCs for the time points indicated. LC3B and p62 protein levels were detected using western blot and relative protein levels calculated as described in materials and methods. HS-5 CM upregulated LC3B-II and p62 protein in PCa cell lines. (B) C4-2B, MDA PCa 2a and MDA PCa 2b PCa cell lines were grown in control growth medium or HS-5 or HS-27a CM in the absence or presence of 40 μM chloroquine (CQ) for two days. CQ led to LC3B-II and p62 accumulation in each growth medium. (C) C4-2, C4-2B, MDA PCa 2a, and MDA PCA 2b PCa cell lines were grown in control growth medium or HS-5 or HS-27a CM for one day. *p62* mRNA levels were determined using QPCR and relative fold mRNA levels graphed. Error bars represent standard deviation of two or three biological replicates. P-value, *≤ 0.05, ** ≤0.005. HS-5 conditioned medium upregulated *p62* mRNA in the PCa cell lines.

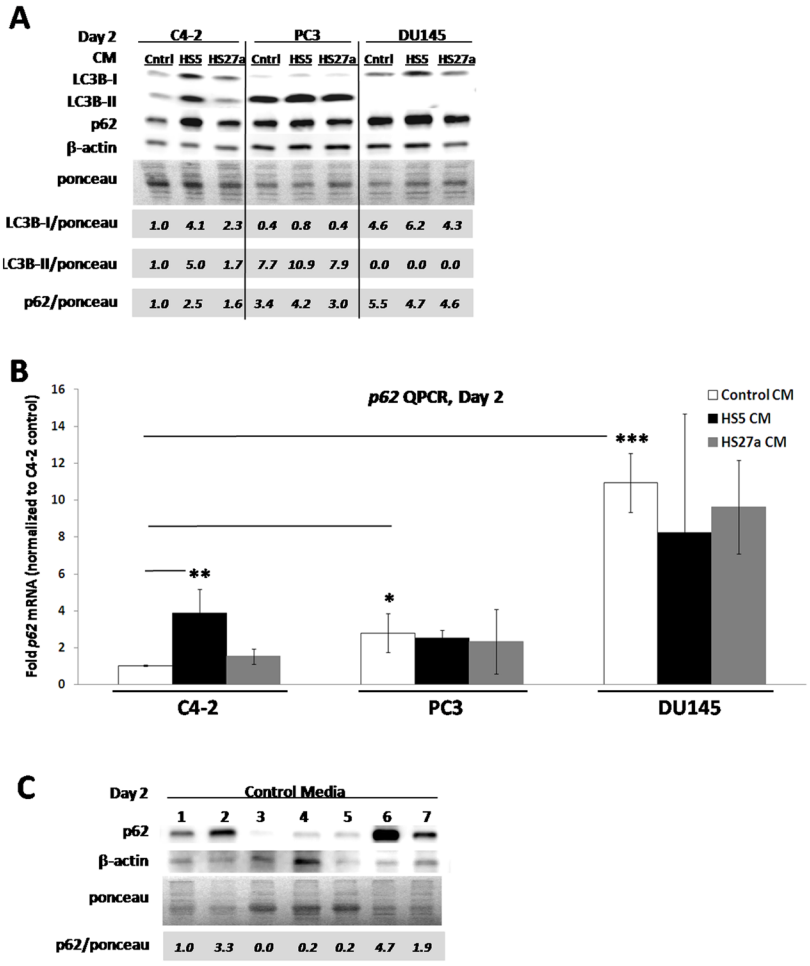

Figure 2. DU145 and PC3 PCa cell lines are less responsive to HS-5-induced accumulation of LC3B-II or p62 and have comparatively high basal p62 accumulation

(A) C4-2, DU145, or PC3 cell lines were grown in control growth medium or HS-5 or HS-27a BMSC conditioned medium (CM) for two days and analyzed by western blot for LC3B and p62. Relative protein levels were determined as described in materials and methods. HS-5 CM upregulated LC3B and p62 protein accumulation in C4-2 cells to a greater extent than in DU145 or PC3 cell lines. However, basal LC3B-II and/or p62 levels were higher in DU145 or PC3 cells than in C4-2 cells. (B) C4-2, DU145, or PC3 cell lines were grown in control growth medium or HS-5 or HS-27a CM for two days. *p62* mRNA levels were determined using QPCR and relative fold mRNA levels graphed. Error bars represent standard deviation of three biological replicates. P-value, *≤ 0.05, ** ≤0.005, ***≤ 0.0005. HS-5 CM upregulated *p62* mRNA in C4-2 cells, but not in DU145 or PC3 cell lines. However, PC3 and DU145 cells showed higher basal *p62* mRNA than C4-2 cells. (C) PCa cell lines were grown in control growth medium for two days. DU145 and PC3 cell lines had comparatively high p62 protein levels.

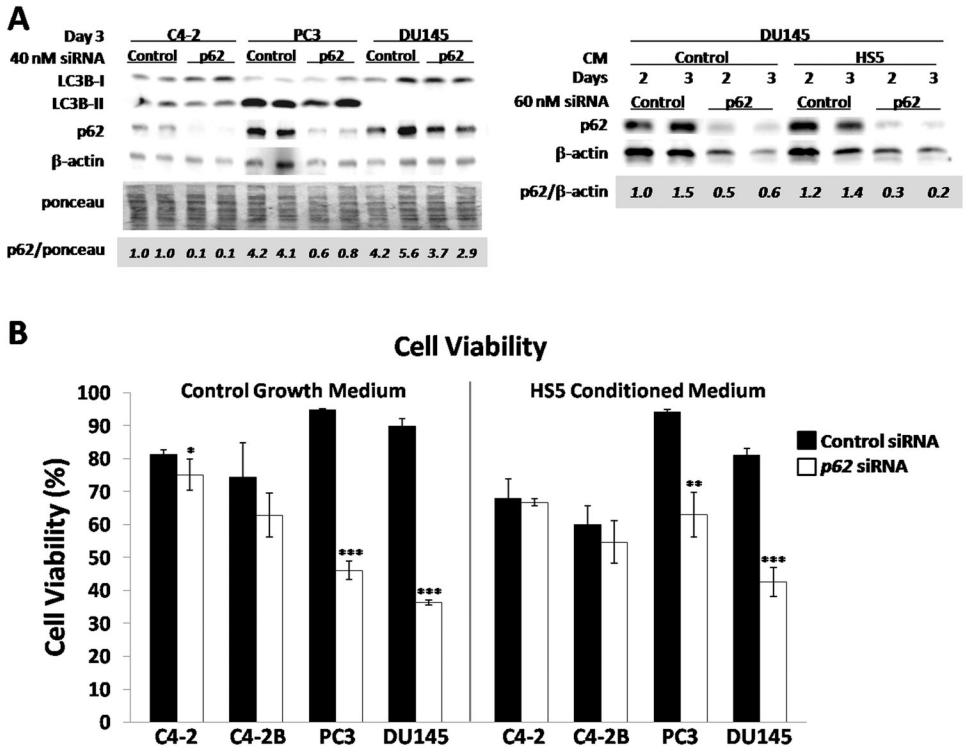

Figure 3. Down regulation of *p62* mRNA is cytotoxic for DU145 and PC3 PCa cell lines

(A) (Left) C4-2, PC3, or DU145 cells were grown in control growth medium in the presence of 40 nM non-target control siRNA or 40 nM *p62* siRNA for three days. LC3B and p62 protein levels were detected using western blot and relative protein levels determined as describe in materials and methods. Two biological replicates are shown for each treatment. Transfection of 40 nM *p62* siRNA was sufficient to reduce p62 protein accumulation to almost undetectable levels in C4-2 and PC3 cells lines, but not in DU145 cells. (Right) DU145 cells grown in control growth medium or HS-5 conditioned medium (CM) were transiently transfected with 60 nM non-target control siRNA or 60 nM*p62* siRNA for two and three days. Transfection of 60 nM *p62* siRNA was sufficient to reduced p62 protein to almost undetectable levels in DU145 cells. (B) C4-2, C4-2B, PC3 and DU145 cells grown in PCa control growth medium or HS-5 CM were transfected with 60 nM non-target control siRNA or 60 nM *p62* siRNA for two days. Live and dead cells were stained with calcein AM and ethidium homodimer 1 (EthD-1) fluorescent dyes, respectively, and live and dead cells were counted to determine cell viability. The error bars represent standard deviation of three biological replicates. P-value, * < 0.05, ** < 0.005, *** <0.0005. *p62* siRNA reduced cell viability more significantly in DU145 and PC3 cells than in C4-2 or C4-2B cells.

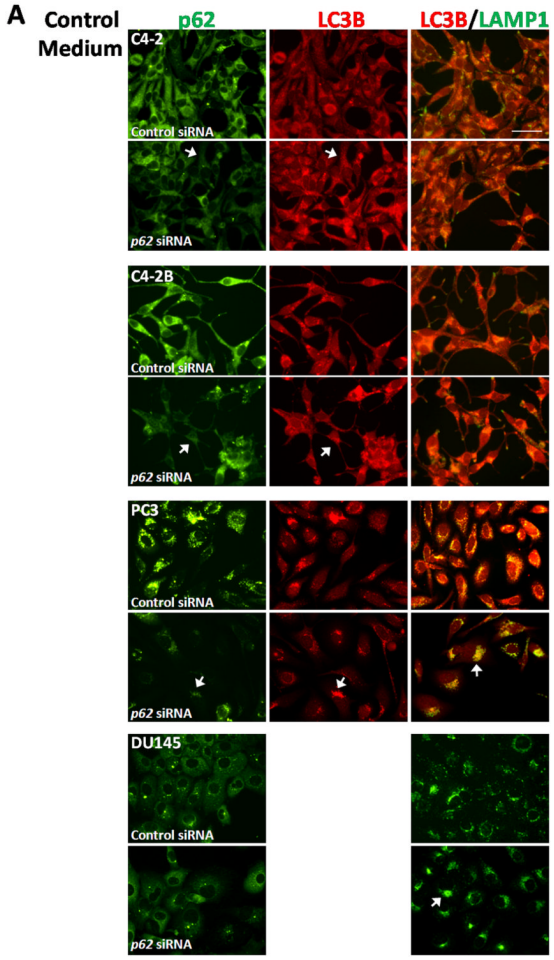

Figure 4. Loss of *p62* alters autolysosome subcellular localization

C4-2, C4-2B, PC3, and DU145 PCa cells were grown in (A) control growth medium or (B) HS-5 conditioned medium (CM) and treated with 60 nM non-target control siRNA or 60 nM *p62* siRNA. After two days, cells were fixed and co-immunostained for p62 (FITC) and LC3B (Texas Red) or LC3B (Texas Red) and LAMP1 (FITC). Immunofluorescent cells were imaged at 40× magnification, scale bar = 100 μm. Shown are matched images of cells co-immunostained for p62 and LC3B and a merged image of cells co-immunostained for LC3B and LAMP1. *p62* siRNA led to loss of total p62 protein in C42, C4-2B, and PC3 cells and loss of p62 puncta in DU145 cells. *p62* siRNA caused peri-nuclear clustering of autolysosome and lysosomes, respectively, in PC3 and DU145 cells (arrow, representative cell). However, in C4-2 or C4-2B cells, *p62* siRNA did not alter subcellular localization of LC3B or LAMP1 when p62 protein levels were reduced (arrow, representative cell).

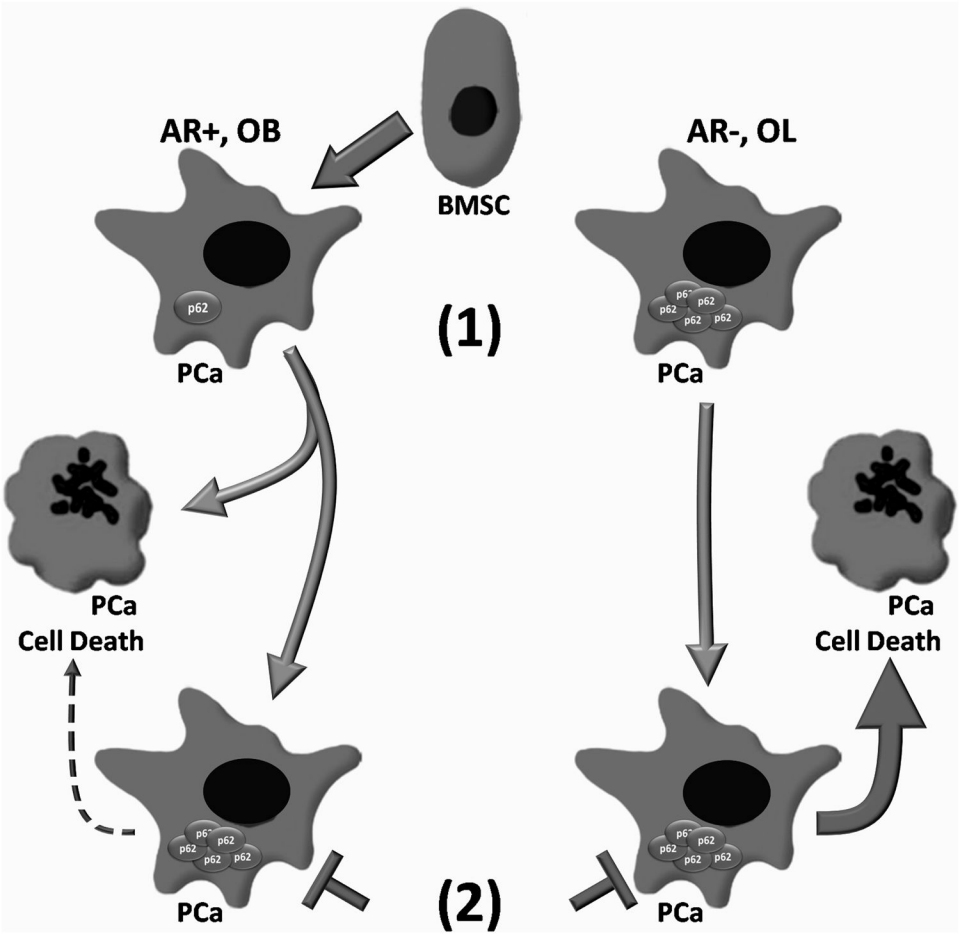

Figure 5. Proposed Model

Based on our data we propose the following model. (1) Prostate cancer (PCa) cells that are androgen receptor positive (AR+) and form largely osteoblastic (OB) lesions represent a PCa subtype that is sensitive to bone marrow stromal cell (BMSC) paracrine induction of PCa apoptosis and induction of autophagy and p62 accumulation in the surviving cell population. PCa cells that are androgen receptor negative (AR-) and form largely osteolytic (OL) lesions represent a PCa cell subtype that has high basal p62 levels and is insensitive to BMSC paracrine-induced PCa apoptosis, autophagy, or p62 upregulation. (2) Loss of p62 (flat arrowhead) is significantly cytotoxic (thick, solid arrow) for BMSC-insensitive PCa cells, indicating that these cells require p62 for survival. Likewise, BMSC-sensitive PCa cells that would escape BMSC-induced apoptosis and colonize the bone would evolve (thin, dashed arrow) into p62-dependent cells due to long-term paracrine induction of p62 accumulation.

Table 1

Cell Line List

Listed are the prostate cancer (above darker line) and bone marrow stromal (below darker line) cell lines used in this study. Cell line phenotypes are described (30-42).

Cell Line	Human Origin	Cell Line Establishment	Tumor Forming Phenotype in Mice	*AR* Expression
C4-2	Lymph node metastasis, 50-year-old Caucasian male.	LNCaP subline isolated from C4 tumor xenograft in castrated mouse. Tumors from lymph node & bone.	Intrailiac or intrafemoral injections; osteoblastic lesions.	Yes
C4-2B	Lymph node metastasis, 50-year-old Caucasian male.	LNCaP subline isolated from C4-2 tumor xenograft in castrated mouse. Tumors isolated from bone.	Intrailiac or intrafemoral injections; osteoblastic lesions.	Yes
MDA PCa 2a & 2b	Bone metastasis, 63-year-old African American male.	2a & 2b are distinct clones from same specimen. 2b cells generate tumors at a higher rate than 2a cells *in vivo*.	Intrafemoral injection of 2b cells; osteoblastic lesions.	Yes
VCaP	Vertebral bone metastasis, 59-year-old Caucasian male.	Passaged as mouse xenograft then cultured *in vitro*.	Intratibial injections; osteoblastic lesions.	Yes
DU145	Brain metastasis, 69-year-old Caucasian male.	Passaged *in vitro*	Injection into human bone xenograft; osteolytic lesions.	No
PC3	Bone metastasis, 62-year-old Caucasian male.	Passaged as mouse xenograft then cultured *in vitro*.	Injection into human bone xenograft; osteolytic lesions.	No
HS-5	Normal bone marrow, 30 year-old Caucasian male.	Bone marrow cells immortalized using LXSN-16 E6E7 retrovirus.	Small fibroblastic cells that secrete higher levels of growth factors than HS27a cells & support hematopoiesis in cell culture.	
HS-27a	Normal bone marrow, 30 year-old Caucasian male.	Bone marrow cells immortalized using LXSN-16 E6E7 retrovirus.	Large flattened epithelioid-like cells that support cobblestone formation of hematopoietic cells in cell culture.	